STATOR HARMONIC CURRENT COMPENSATION METHOD FOR DFIG CONNECTED TO A DISTORTED GRID THROUGH PROPER ADJUSTMENT OF LINEAR ROTOR CURRENT CONTROLLERS

Gustavo Gontijo*, Thiago Tricarico*, Felipe Dicler*, Matheus Soares*, Leonardo Silva*, Mauricio Aredes*

*Federal University of Rio de Janeiro
Rio de Janeiro, RJ, Brazil

Emails: gustavo@lemt.ufrj.br, thiago@lemt.ufrj.br, dicler@lemt.ufrj.br, matheussoares@lemt.ufrj.br, leonardo@lemt.ufrj.br, aredes@lemt.ufrj.br

Abstract— The DFIG is highly attractive to the wind power industry due to its technical and economic advantages. However, the fact that its stator is directly connected to the electrical grid leads to serious power quality issues that are making the DFIG market share reduce, considerably, in the last few years. For instance, if the grid voltage is distorted the generator stator current will be distorted leading to loss in the system efficiency, to undesired torque pulsations and the system might be unable to comply with grid codes regarding harmonic current injection. Many different control strategies and converter topologies have been proposed aiming at mitigating these harmonic currents. Most of the techniques are based on the addition of extra, dedicated controllers besides the usual linear controllers that regulate the rotor current fundamental component. This paper develops a stability analysis, based on the linear control theory, aiming at designing the usual rotor current controllers in such a way that they are enough to compensate for stator harmonic current components. In other words, the linear controllers will be designed so that they have a frequency response characteristic that both maintain their good dynamic behavior and compensate for stator harmonic currents.

Keywords— DFIG, stability analysis, harmonic current compensation.

Resumo— O DFIG é uma opção de topologia altamente requisitada pela indústria eólica devido às suas vantagens técnicas e econômicas. No entanto, o fato de seu estator estar diretamente conectado ao sistema elétrico acarreta em graves questões de qualidade de energia que estão levando a uma considerável diminuição na parcela de mercado do DFIG, nos últimos anos. Por exemplo, se a tensão da rede for distorcida, a corrente de estator do gerador será distorcida acarretando em perda de eficiência, em indesejáveis pulsações de torque e o sistema pode se tornar incapaz em cumprir normas de rede relacionadas ao conteúdo harmônico de corrente. Muitas diferentes estratégias de controle e topologias de conversores foram propostas visando a mitigação destas correntes harmônicas. A maioria das técnicas de controle são baseadas na adição de controladores dedicados extras além dos controladores lineares convencionais que regulam a componente fundamental da corrente de rotor. Este artigo desenvolve uma análise de estabilidade, baseada na teoria de controle linear, visando o projeto dos controladores de corrente de rotor convencionais de modo que estes sejam suficientes para a compensação de correntes harmônicas de estator. Em outras palavras, os controladores lineares serão projetados de modo a possuírem uma característica de resposta em frequência que mantenha o bom desempenho dinâmico do controle de componente fundamental e compense correntes harmônicas de estator.

Palavras-chave— DFIG, análise de estabilidade, compensação de correntes harmônicas.

1 Introduction

The doubly-fed induction generator (DFIG) is still one of the most used wind system topologies, despite the considerable growth of the use of the permanent-magnet synchronous generator (PMSG), led by the current trend of offshore wind farms (Olloqui et al., 2016). The high interest of the wind industry in the DFIG is due to its many technical and economic advantages. However, some drawbacks deserve attention such as the fact that its stator is directly connected to the grid leading to power quality issues. Harmonic voltage components are common in weak distribution grids, to which the wind farms are usually connected. This voltage profile leads to a harmonic current flow through the DFIG stator windings towards its rotor. These currents lead to an increase in the losses in the copper wires, as well as in the iron core. Besides, undesirable torque pulsations will occur and the system might not be able to comply with grid codes (Liu et al., 2012; Gontijo, Tricarico, Krejci, Guedes, França and Aredes, 2017; Chen et al., 2012; Gontijo, Tricarico, Krejci, França and Aredes, 2017).

Many different converter topologies (Datta et al., 2015; Gontijo, Tricarico, Krejci, França and Aredes, 2017) and control strategies (Liu et al., 2012; Gontijo, Tricarico, Krejci, Guedes, França and Aredes, 2017; Chen et al., 2012; Hu et al., 2011; Hu et al., 2009; Nguyen et al., 2012; Nian et al., 2015; Hu et al., 2013; Wu and Nian, 2018; Cheng and Nian, 2017) have been proposed in order to solve this power quality problem. In (Datta et al., 2015; Gontijo, Tricarico, Krejci, França and Aredes, 2017), the authors use series-grid-side converters (SGSC) in order to compensate for stator harmonic voltages and, thus, stator harmonic currents. In (Cheng and Nian, 2017), a model predictive stator current control (MPSCC) is used to compensate for stator harmonic currents.

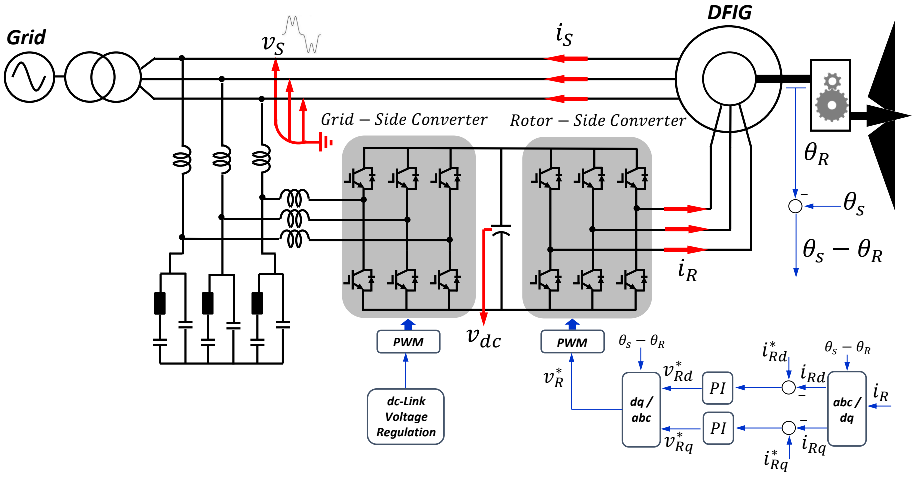

Figure 1: DFIG system topology.

However, most of the mentioned control strategies, aiming at mitigating stator harmonic currents, are based on the addition of special dedicated controllers to perform this task besides the usual rotor-current-fundamental-component controllers. The technique works by synthesizing a rotor voltage with the harmonic content of the DFIG terminal voltage in order to make the rotor a high-impedance path, blocking the harmonic currents flowing through the generator stator towards its rotor. In (Liu et al., 2012; Gontijo, Tricarico, Krejci, Guedes, França and Aredes, 2017), additional resonant controllers are used to directly control the stator current in order to achieve harmonic compensation. In (Hu et al., 2011; Hu et al., 2009; Nian et al., 2015; Hu et al., 2013), dedicated resonant controllers are used to control the rotor currents, aiming at mitigating the slip components related to the stator current harmonic components, leading to a sinusoidal stator current. In (Chen et al., 2012; Nguyen et al., 2012), additional dedicated linear controllers are used to obtain the compensation. This is possible because the measured currents are referred to rotating reference frames with angular speeds related to the stator-current-harmonic-components frequencies. In (Wu and Nian, 2018), a feedforward technique is used to achieve the desired compensation.

This paper proposes a proper adjustment of the usual linear rotor current controllers, in order to achieve stator harmonic current compensation, with no need of additional dedicated controllers. The controllers are designed using the linear control theory and setting the parameters of bandwidth, phase margin and open-loop amplitude gain in order to achieve good dynamic behavior and stator harmonic current compensation. To the best of the authors' knowledge, this analysis and compensation technique have not been reported in the literature thus far, since the reported papers always suggest the use of additional dedicated controllers.

2 Stator harmonic current compensation control strategy

The block diagram of the control strategy adopted in this paper is depicted in Figure 1, which is composed by the control of the grid-side converter, aiming at regulating the dc-link voltage (v_{dc}), and by the control of the rotor-side converter, responsible for the generator speed regulation and for the stator reactive power injection, by providing the direct-axis (i_{Rd}^*) and in-quadrature-axis (i_{Rq}^*) rotor current references, respectively. The rotor-side converter control is realized in a dq-rotating reference frame with the slip angular speed ($\omega_s - \omega$), in such a way that the rotor current fundamental component is constant, in this reference frame, and the control can be realized with linear proportional-integral (PI) controllers. ω_s and ω are the grid voltage synchronous angular speed and rotor angular speed, respectively and θ_R and θ_s are the measured rotor angle and the stator voltage angle, respectively. θ_s is obtained through a PLL.

If the grid voltage is distorted, harmonic currents will flow through the DFIG stator. The stator current (i_S) will be composed by a space vector of fundamental component, rotating with angular speed related to the grid fundamental frequency (ω_s), and by space vectors related to the grid voltage harmonic components rotating with angular speeds related to the grid harmonic frequencies ($k\omega_s$), in which $k = 5, 7, 11....$ This current will flow towards the generator rotor. The rotor current fundamental component will be represented by a space vector rotating with angular speed related to the slip frequency equal to $\omega_s - \omega$. The rotor current harmonic components will be represented by space vectors rotating with angular speeds equal to $k\omega_s - \omega$. Since the control is realized in the dq-rotating reference frame with angular speed equal to $\omega_s - \omega$, the rotor current fundamental component is a dc component, in this reference $((\omega_s - \omega) - (\omega_s - \omega) = 0$ rad/s), and the rotor current harmonic components are represented by space vectors that rotate with angular speeds equal to $(k\omega_s - \omega) - (\omega_s - \omega) = (k-1)\omega_s$, in the dq-rotating reference frame.

The PI current controllers have an open-loop-frequency-response characteristic of infinite gain to dc components and, thus, produce a null error in closed-loop, meaning that the references are properly tracked. Furthermore, if these linear controllers are designed in such a way to have an open-loop-frequency-response characteristic with high enough gain, for the frequencies of the rotor current harmonic components, the rotor voltage references (v^*_{Rd} and v^*_{Rq}), that are responsible for the synthesized rotor voltage (v_R), will be composed by not only fundamental component, but also some harmonic content, diminishing the closed-loop error between the rotor current harmonic components and a null reference. This rotor voltage profile will act in opposition to the machine terminal voltage, blocking the harmonic current flow. Thus, the DFIG steady-state equivalent circuit can be described as depicted in Figure 2, in which the stator current (i_S) and the rotor current (i_R) are sinusoidal, even though the stator voltage (v_S) is distorted. In Figure 2, L_{lS}, L_{lR} and L_M are the stator leakage, rotor leakage and magnetizing inductances, respectively. R_R and R_S are the rotor and stator resistances, respectively. S is the generator slip.

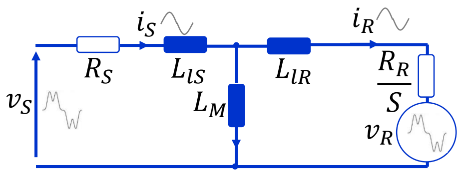

Figure 2: DFIG equivalent circuit with harmonic compensation.

3 DFIG mathematical model

The DFIG linear model, represented by a transfer function with the rotor voltage (v_R) as an input and the rotor current (i_R) as an output, can be obtained through the following equations that describe the machine parameters in a dq-synchronous reference frame (Paul C. Krause and Sudhoff, 2002):

$$v_{Rd} = R_R i_{Rd} + \frac{d}{dt}\lambda_{Rd} - \omega_{slip}\lambda_{Rq} \quad (1)$$

$$v_{Rq} = R_R i_{Rq} + \frac{d}{dt}\lambda_{Rq} + \omega_{slip}\lambda_{Rd} \quad (2)$$

$$v_{Sd} = R_S i_{Sd} + \frac{d}{dt}\lambda_{Sd} - \omega_s\lambda_{Sq} \quad (3)$$

$$v_{Sq} = R_S i_{Sq} + \frac{d}{dt}\lambda_{Sq} + \omega_s\lambda_{Sd} \quad (4)$$

$$\begin{bmatrix}\lambda_{Rd}\\ \lambda_{Rq}\\ \lambda_{Sd}\\ \lambda_{Sq}\end{bmatrix} = \begin{bmatrix} L_R & 0 & L_M & 0\\ 0 & L_R & 0 & L_M\\ L_M & 0 & L_S & 0\\ 0 & L_M & 0 & L_S\end{bmatrix}\begin{bmatrix} i_{Rd}\\ i_{Rq}\\ i_{Sd}\\ i_{Sq}\end{bmatrix} \quad (5)$$

In which $L_S = L_{lS} + L_M$, $L_R = L_{lR} + L_M$ and $\omega_{slip} = \omega_s - \omega$. Also, λ_R and λ_S are the rotor and stator flux linkages, respectively.

Using algebraic manipulations and referring the parameters to the Laplace s-domain, the following transfer function can be obtained, if disturbances are neglected (Murari et al., 2017; Liu et al., 2012; Chen et al., 2012):

$$\frac{i_{Rd}}{v_{Rd}} = \frac{1}{(L_R\sigma)s + R_R} \quad (6)$$

In which:

$$\sigma = 1 - \frac{L_M^2}{L_S L_R} \quad (7)$$

Furthermore, the generator electromagnetic torque, in a stator voltage oriented control (SVOC) strategy, can be obtained as follows (Bin Wu and Kouro, 2011):

$$T_e = \frac{3pL_M v_{Sd}}{2\omega_s L_S} i_{Rd} \quad (8)$$

In which T_e is the electromagnetic torque, p is the number of pole pairs of the turbine. In Figure 3, the entire linear model that can be used to develop the control project of a DFIG operating under a SVOC, in order to realize speed control, is depicted. In this paper, this control is composed by three PI controllers in a cascade configuration. The block diagram is composed by a converter model, the DFIG model presented in (6), the torque estimation block presented in (8) and a mechanical model, besides the controllers.

4 Stability analysis

In this paper, a stability analysis is carried out in order to prove the effectiveness of using the linear rotor current controllers (inner control loop in Figure 3) to obtain stator harmonic current compensation besides regulating the rotor current fundamental component. In Figure 4, the block diagram used for the analysis is shown. In this figure, the transfer function $G(s)$ is composed by the DFIG linear model along with the converter model and the transfer function $H(s)$ is composed by $G(s)$ along with the linear current controller.

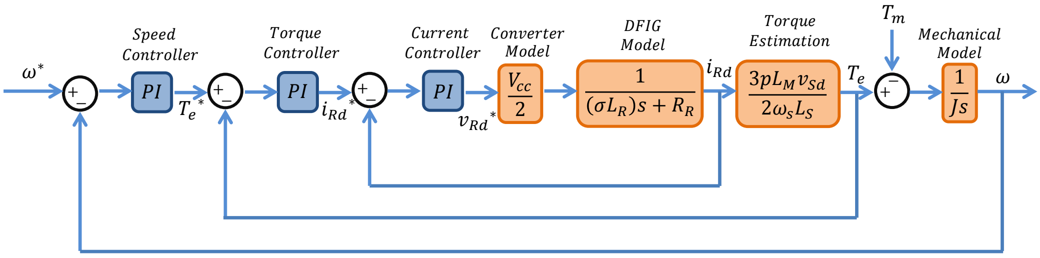

Figure 3: Control project mathematical model.

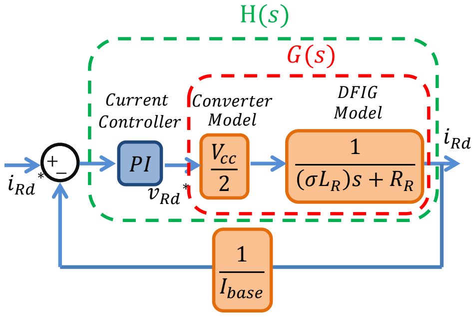

Figure 4: Mathematical model for stability analysis.

In this analysis, four different controllers are used leading to four different open-loop transfer functions ($H_1(s), H_2(s), H_3(s)$ and $H_4(s)$). In Figure 4, I_{base} represents the current base used to convert the rotor current to a per unit value.

The parameters of the four different current controllers were selected aiming at obtaining different frequency responses characteristics and time domain behavior, in order to show that both proper dynamic behavior and harmonic current compensation can be obtained, depending on the parameters selection. These parameters are shown in Table 1.

Table 1: PI Current Controllers Parameters.

Transfer Function	kp	ki
$H_1(s)$	0.20	1000
$H_2(s)$	0.75	247
$H_3(s)$	2.56	7924
$H_4(s)$	9.01	1266

Supposing that an arbitrary system, as depicted in Figure 5, has an open-loop gain equal to $A = |H(j\omega_f)|$, for a given frequency of interest with angular speed corresponding to ω_f. Then, its closed-loop error ($E(j\omega_f)$) can be calculated as follows:

$$E(j\omega_f) = U(j\omega_f) - Y(j\omega_f) \quad (9)$$

In which:

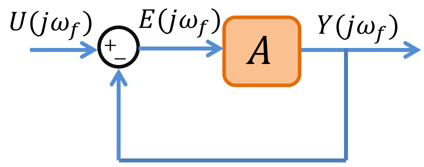

Figure 5: Arbitrary closed-loop transfer function.

$$Y(j\omega_f) = AE(j\omega_f) \quad (10)$$

By substituting (10) into (9), the following expression can be obtained:

$$E(j\omega_f) = \frac{1}{1+A}U(j\omega_f) \quad (11)$$

By analyzing (11), one can notice that the higher the open-loop gain (A) is, the lower the closed-loop error ($E(j\omega_f)$), between the reference input signal ($U(j\omega_f)$) and the output signal ($Y(j\omega_f)$), will be, in steady-state for the frequency of interest with angular speed equal to ω_f.

In Figure 6, the open-loop bode plots for each of the transfer functions $H(s)$, with controller parameters presented in Table 1, are depicted. In the magnitude plot there is a red line showing the angular speed equal to 2262 rad/s, which corresponds to the frequency 360 Hz. Both positive-sequence $7th$ harmonic component (420 Hz) and negative-sequence $5th$ harmonic component (300 Hz), present in the stator current, will induce rotor currents with frequency equal to 360 Hz, in the dq-rotating reference frame. This fact can be properly understood remembering that the rotor current harmonic components space vectors, in the dq-rotating reference frame, have angular speed equal to $(k-1)\omega_s$, as previously mentioned. Since the 5_{th} harmonic is a negative-sequence component, its space vector angular speed, in the dq-rotating reference frame, is equal to $|\omega_5^-| = |(-5-1)\omega_s| = 6\omega_s = 2262$ rad/s, considering that $\omega_s = 377$ rad/s. Equivalently, $|f_5^-| = |(-300$ Hz$) - (60$ Hz$)| = 360$ Hz. Besides, the 7_{th} harmonic is a positive-sequence component, its space vector angular speed, in the dq-rotating reference frame, is equal to $|\omega_7| = |(7-1)\omega_s| = 6\omega_s = 2262$

rad/s. Equivalently, $|f_7| = |(420 \text{ Hz}) - (60 \text{ Hz})| = 360$ Hz.

By analyzing Figure 6, it can be seen that each of the transfer functions has different open-loop gains at the frequency equal to 2262 rad/s.

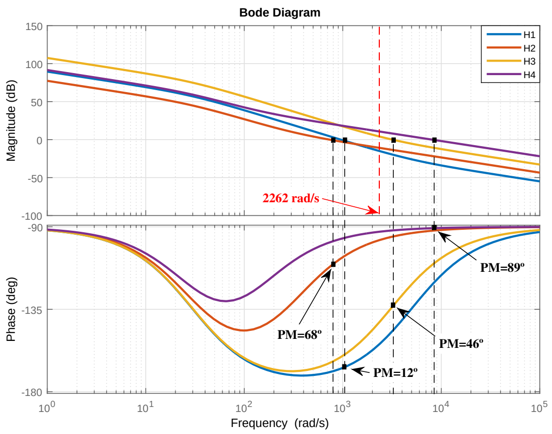

Figure 6: Open-loop Bode plot for compensation and stability analysis.

By analyzing Figure 6, one can notice that $H_4(s)$ is the transfer function that provides the smaller error between the output rotor current and a null input reference, at the frequency of 360 Hz. In other words, $H_4(s)$ is the transfer function with the highest open loop gain for the frequency of interest $\omega_f = 2262$ rad/s. Besides, this is also the transfer function with higher phase-margin ($PM = 89^0$) resulting in a highly-damped system. In Figure 7, one can notice the connection between the open-loop Bode plot phase-margins and the closed-loop Bode plot resonance peaks, which are related to the system damping constant.

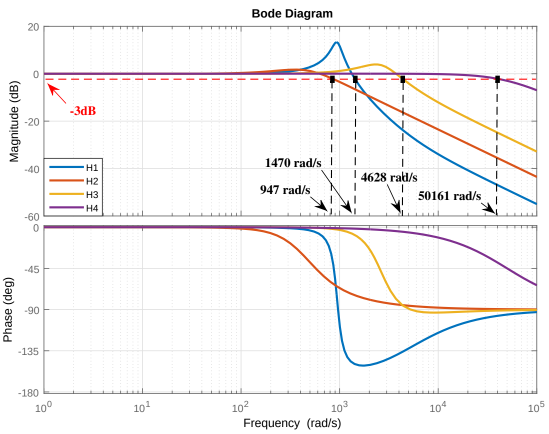

Figure 7: Closed-loop Bode plot for compensation and stability analysis.

It is important to notice that $H_1(s)$ is poorly damped, with the highest resonance peak and this fact can be further analyzed by observing Figure 8, in which a step response plot is depicted for each of the transfer functions. The transfer function $H_4(s)$ besides being the one that provides the highest open-loop gain, for the desired frequency, is also the most damped one and the one with faster dynamic behavior, which can also be confirmed by observing its bandwidth (50161 rad/s), depicted in Figure 7.

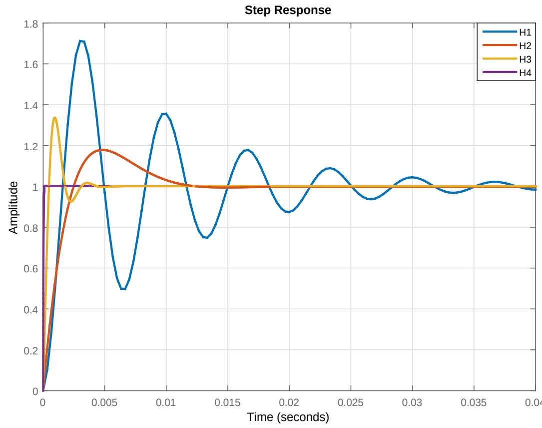

Figure 8: Step responses for time domain analysis.

By comparing the open-loop gains and phase-margins, and closed-loop resonance peaks and bandwidths, between the transfer functions $H_2(s)$ and $H_3(s)$, one can notice that $H_3(s)$ provide higher harmonic compensation and has faster dynamic behavior, even though $H_2(s)$ has better damping. Thus, by analyzing Figure 6, 7 and 8, one can conclude that the linear current controllers parameters can be optimized in order to fulfill the project requirements regarding damping, dynamic behavior and harmonic compensation functionality.

5 Simulation results

In this paper, four different simulations were carried out using the software PSCAD/EMTDC. Each of the simulations are related to one of the four different transfer functions $H(s)$. A 18.810 kVA DFIG with rated voltage equal to 380 V is driven by a wind turbine model. The wind system is connected to a grid with voltage distortion corresponding to 7% of 5^{th} harmonic and 5% of 7^{th} harmonic. In Figure 9, the steady-state stator and rotor current waveforms, for each of the transfer functions $H(s)$, are depicted. These waveforms demonstrate the harmonic current compensation functionality.

By analyzing Figure 9, it becomes clear that the desired harmonic current compensation could be achieved by properly designing the linear current controllers. In Figures 9(a) and (b), the stator and rotor currents corresponding to the transfer function $H_1(s)$ are shown, respectively. Figures 9(c) and (d), (e) and (f), (g) and (h) show the stator and rotor currents corresponding to the transfer functions $H_2(s)$, $H_3(s)$ and $H_4(s)$, respectively. These figures show the compensation achieved due to the open-loop gain of each of the transfer functions, as described in Figure 6. In other words, the higher the open-loop gain of the given transfer function $H(s)$, at the desired frequency (360 Hz or 2262 rad/s), the smaller the presence of the 5^{th} (300 Hz) and 7^{th} (420 Hz) harmonic components in the respective stator current waveform and the smaller the 360 Hz component in the respective rotor current waveform. It can be seen that both stator and rotor currents are highly sinusoidal for the transfer function $H_4(s)$. The linear current controllers are able to actuate at the harmonic components frequencies, generating a rotor voltage with some harmonic content, which blocks the harmonic currents flowing through the machine stator and rotor windings.

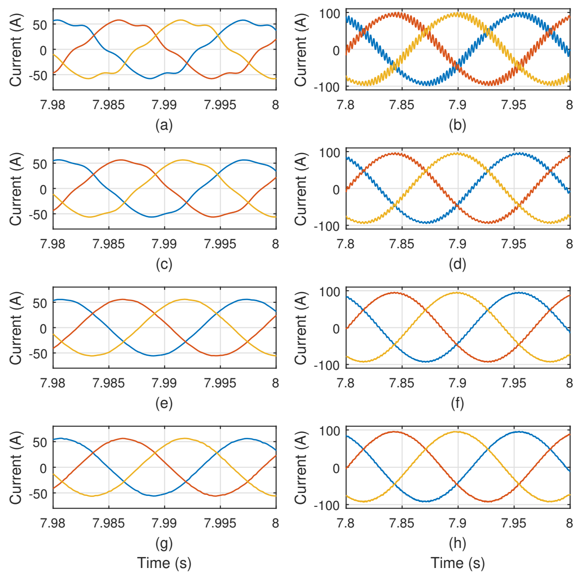

Figure 9: Current waveforms for each transfer function $H(s)$. (a) stator current for $H_1(s)$, (b) rotor current for $H_1(s)$, (c) stator current for $H_2(s)$, (d) rotor current for $H_2(s)$, (e) stator current for $H_3(s)$, (f) rotor current for $H_3(s)$, (g) stator current for $H_4(s)$, (h) rotor current for $H_4(s)$.

6 Conclusions

In this paper, a DFIG harmonic current compensation strategy is proposed by properly adjusting the usual linear rotor current controllers so that they are able to actuate at harmonic frequencies, thus synthesizing a rotor voltage profile that besides regulating the generator speed, blocks the harmonic current that would flow through the machine stator towards its rotor.

Acknowledgements

The authors would like to thank FAPERJ for the financial support.

References

Bin Wu, Yongqiang Lang, N. Z. and Kouro, S. (2011). *Power Conversion and Control Of Wind Energy Systems*, IEEE Press.

Chen, W., Xu, J., Zhu, N., Liu, C., Chen, M. and Xu, D. (2012). Stator harmonic current suppression for dfig wind power system under distorted grid voltage. Proceedings - 2012 3rd IEEE International Symposium on Power Electronics for Distributed Generation Systems, PEDG 2012.

Cheng, C. and Nian, H. (2017). Low-complexity model predictive stator current control of dfig under harmonic grid voltages. IEEE Transactions on Energy Conversion.

Datta, S., Mishra, J. P. and Roy, A. K. (2015). Unbalance and non-linear stator voltage control of a grid connected dfig based wecs using nsc. 12th IEEE International Conference Electronics, Energy, Environment, Communication, Computer, Control: (E3-C3), INDICON 2015.

Gontijo, G., Tricarico, T., Krejci, D., França, B. and Aredes, M. (2017). A novel stator voltage distortion and unbalance compensation of a dfig with series grid side converter. 4th Brazilian Power Electronics Conference -COBEP2017.

Gontijo, G., Tricarico, T., Krejci, D., Guedes, S., França, B. and Aredes, M. (2017). Stator harmonic current compensation of a dfig connected to a grid with voltage distortion. 4th Brazilian Power Electronics Conference -COBEP2017.

Hu, J., He, Y., Xu, L. and Williams, B. W. (2009). Improved control of dfig systems during network unbalance using pi-r current regulators. IEEE Transactions on Industrial Electronics.

Hu, J., Nian, H., Xu, H. and He, Y. (2011). Dynamic modeling and improved control of dfig under unbalanced and distorted grid voltage conditions. IEEE Transactions on Energy Conversion.

Hu, J., Xu, H. and He, Y. (2013). Coordinated control of dfig's rsc and gsc under generalized unbalanced and distorted grid voltage conditions. IEEE Transactions on Industrial Electronics.

Liu, C., Blaabjerg, F., Chen, W. and Xu, D. (2012). *Stator Current Harmonic Control With Resonant Controller for Doubly Fed Induction Generator*. IEEE Transactions on Power Electronics.

Murari, A. L. L. F., Altuna, J. A. T., Jacomini, R. V., Osorio, C. M. R., Chaves, J. S. S. and Filho, A. J. S. (2017). A proposal of project of pi controller gains used on the control of doubly-fed induction generators. IEEE Latin America Transactions.

Nguyen, N.-T., Chun, T.-W. and Lee, H.-H. (2012). An enhanced control algorithm for stand-alone dfig system feeding unbalanced loads with reduced current sensors. Conference Proceedings - 2012 IEEE 7th International Power Electronics and Motion Control Conference - ECCE Asia, IPEMC 2012.

Nian, H., Cheng, P. and Zhu, Z. Q. (2015). Independent operation of dfig-based wecs using resonant feedback compensators under unbalanced grid voltage conditions. IEEE Transactions on Power Electronics.

Olloqui, A., Elizondo, J. L., Rivera, M., Macías, M. E., Micheloud, O. M., Peña, R. and Wheeler, P. (2016). *Modulated Model Predictive Rotor Current Control (M2PC) of a DFIG Driven by an Indirect Matrix Converter With Fixed Switching Frequency*. 2016 IEEE 2nd Annual Southern Power Electronics Conference, SPEC 2016.

Paul C. Krause, O. W. and Sudhoff, S. D. (2002). *Analysis of Electric Machinery and Drive Systems*, second edition edn, Scribner.

Wu, C. and Nian, H. (2018). Stator harmonic currents suppression for dfig based on feedforward regulator under. IEEE Transactions on Power Electronics.